IEEE Access
Multidisciplinary | Rapid Review | Open Access Journal

Received November 16, 2018, accepted January 15, 2019, date of current version March 5, 2019.

Digital Object Identifier 10.1109/ACCESS.2019.2899400

Strength Analysis of the Main Structural Component in Ship-to-Shore Cranes Under Dynamic Load

GANG TANG[1,2], CHEN SHI[1,2], YIDE WANG[2], AND XIONG HU[1]
[1]Logistics Engineering College, Shanghai Maritime University, Shanghai 201306, China
[2]Université de Nantes IETR, UMR CNRS 6164, 44035 Nantes, France

Corresponding authors: Chen Shi (shichen77@qq.com) and Xiong Hu (huxiong@shmtu.edu.cn)

This work was supported in part by the National Natural Science Foundation of China under Grant 31300783, in part by the China Postdoctoral Science Foundation under Grant 2014M561458, in part by the Doctoral Fund of the Ministry of Education Jointly Funded Project under Grant 20123121120004, in part by the Shanghai Maritime University Research Project under Grant 20130474, in part by the Shanghai Top Academic Discipline Project Management Science and Engineering, and in part by the High-Tech Research and Development Program of China under Grant 2013A2041106.

ABSTRACT After a period of operation, the mechanical properties of ship-to-shore (STS) cranes can change. It is necessary to analyze the strength of the main structural component in STS cranes under dynamic load to assess their safety. This case study was conducted on a 28-ton capacity STS crane. A testing system with signal sensing, conditioning, acquiring, and analysis was established. After on-site testing, all of the stresses of the test positions were calculated and determined to be in the allowable range. As a result of this paper, a systematic approach to analyze the strength of the main structural component in STS cranes under dynamic load is proposed.

INDEX TERMS Ship-to-shore cranes, dynamic load, Kalman filter.

I. INTRODUCTION

Ship-to-shore (STS) cranes are used in ports and terminals to transfer containerized cargo to and from ships [1]. Since its inception more than 50 years ago (the first quayside container crane was built in January 1959 [2]), the container industry has made remarkable progress. The typical elements of an STS crane include a combination of two sets of ten rail wheels mounted to the bottom of the vertical frame and braced system; a structurally designed system of beams assembled to support the boom, cabin, operating machinery, and the cargo being lifted; crane boom; hook; operating cabin; and storage equipment. The crane is driven by a specially trained operator who sits in a cabin attached to the trolley suspended from the beam. The trolley runs along rails located on the top or sides of the boom and girder. The operator runs the trolley over the ship to lift the cargo, usually containers. Once the spreader locks onto the container, the container is lifted, moved over the dock, and placed on a truck chassis (trailer) to be taken to the storage yard. The crane also lifts containers from the chassis on the dock to load them onto the ship.

STS cranes are mostly used for a long duration. Prolonged use affects the mechanical properties of STS cranes. If an accident occurs, the economic losses can be enormous, and thus, safety assessments are necessary. There are many performance indicators related to STS crane safety, including structure strength, dynamic stiffness, and fatigue strength. The main objective of this paper is to study the strength of the main structural component in STS cranes under dynamic load.

There are many studies on machines under dynamic load. For example, a simple experimental technique employing wire strain gauges for measuring dynamic loads and stresses in operating gear systems has been described in [3]. Others have applied simple rigid-plastic methods to analyze plastic failure of ductile beams loaded dynamically, such as Jones in [4]. Laman *et al.* [5] have calculated the dynamic load allowance in steel through-truss bridges. Shenoy and Fatemi [6] have performed quasi-dynamic finite element analysis (FEA) for a typical connecting rod to capture stress variations over a cycle of operation. Hwang and Nowak [7]

The associate editor coordinating the review of this manuscript and approving it for publication was Shuai Liu.

2169-3536 © 2019 IEEE. Translations and content mining are permitted for academic research only.
Personal use is also permitted, but republication/redistribution requires IEEE permission.
See http://www.ieee.org/publications_standards/publications/rights/index.html for more information.

have analyzed the simulation of dynamic loads in bridges. Kopnov [8] has predicted the fatigue life of the metalwork of a travelling gantry crane. Some experiments on a welded steel frame exposed to fatigue loading, and on wire ropes damaged by saw cuts have been conducted in [9]. Research about the sensitivity of some sources of uncertainty in the seismic response of a Korean container crane structure has been reported in [10]. A comparative study of nonlinear static and time history analyses of typical Korean STS container cranes has been provided in [11]. Furthermore, there are some published books about the impact strength of materials [12] and providing some examples of structural computation of machine components [13]. However, in the existing literature, we have not found a systematic testing approach applied to STS cranes under dynamic load.

In this paper, the dynamic load strength test is designed to determine whether the main structural component of an STS crane can withstand transient impact stresses caused by preset loads and changes in the trolley position. Using the worst possible working conditions allows us to determine whether the structure meets strength requirements. In this paper, a study on an STS crane with 28-ton capacity and 18 years of service has been conducted with on-site testing. We have not conducted field tests under strong wind conditions because of safety concerns [14].

The remainder of the paper is organized as follows. In section II, we introduce the test method, including the principles of the testing system, the location of measuring points to find the loading, and the conditions. In section III, we summarize the data and analyze it with Kalman filter, showing the maximum value of stress at each measuring point. In section IV, we present our conclusions.

II. TESTING METHOD

A. TESTING SYSTEM

The dynamic load test assesses the dynamic loading stresses in the main girder carrying the member system, rod system, and gantry system. Tensile stress is expressed as positive while compressive stress is negative. Figure 1 shows a schematic structure of our dynamic load strength test and analysis. It includes strain measuring points, signal sensing and conditioning, signal analysis, and output. The signals enter a 14-channel strain gauge signal conditioner to be processed and amplified. One of the advantages of this testing system is that it can produce a stable gauge output signal. Using the on-site data acquisition system, the parameters of the dynamic load working condition can be obtained. These data and synchronously processed signals will be stored in the specified virtual instrument memory for the secondary processing.

Dynamic load stress testing and analysis of the main equipment will use the following instruments and sensors:

1) electrical resistance strain gauges,
2) quad strain adapter, and
3) crane status monitoring and evaluation system, which mainly includes

   a) workstation,
   b) signal channel expansion box,
   c) signal conditioning apparatus,
   d) data collector,
   e) visualization software, and
   f) data management and analysis software.

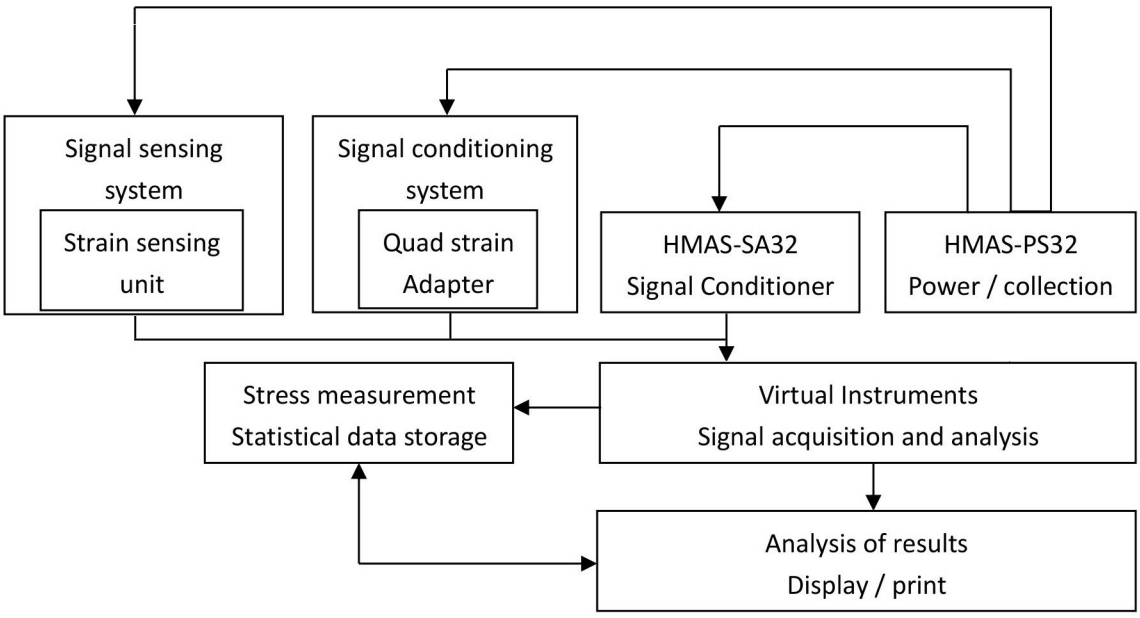

FIGURE 1. Flow chart of the testing system.

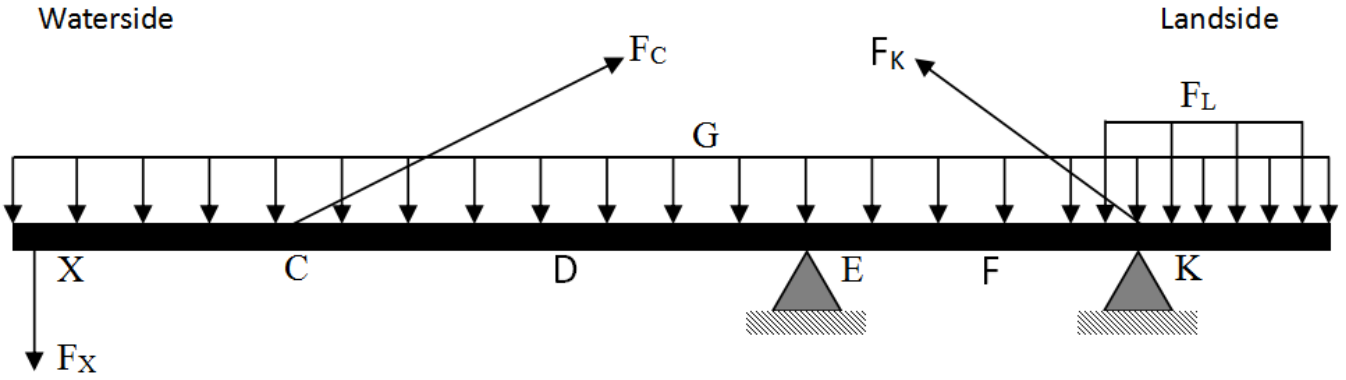

FIGURE 2. Reaction for the beam. F_X : Dynamic load (Self-weight of trolley and hopper, and test load); F_C : Force of the diagonal link reaction on point C; F_L : Weight of the house (Machinery house, electric room, power station and so on); G : Self-weight of the beam; D : Center between C and E; F : Center between E and K. F_K : Force of the diagonal link reaction on point K.

B. MEASURING POINTS

The beam of an STS crane is primarily subjected to transverse and axial loads. When we analyze the strength of the main structural component, we ignore axial loads. Consider a beam that is simply-supported at E and K, and subjected to three concentrated loads and two distributed loads as shown in Figure 2. F_x is the dynamic load acting on the beam; the location of X can be changed along the beam.

The transverse loads cause internal shear forces and bending moments, which in turn cause axial stresses and shear stresses in the cross section. Considering the reactions as plane stress states, we obtain the following empirical equation for calculating the total stress [15]:

$$\sigma = \sqrt{\sigma_1^2 + \sigma_m^2 - \sigma_1\sigma_m + 3\tau^2} \tag{1}$$

where σ_1 is the longitudinal axial stress caused by the bending moment, σ_m is the compressive stress caused by the concentrated load, and τ is the shear stress. The simple theory of elastic bending states that

$$\sigma_1 = \frac{M_{max}}{Z} \tag{2}$$

where M_{max} is the maximum bending moment for the beam and Z is the section modulus. If the force is evenly distributed across the cross section, the internal forces can be approximated as uniform, and the beam is subjected to a uniform normal stress, defined as

$$\sigma_m = \frac{P}{\delta_i C} \tag{3}$$

with P the concentrated load, δ_i the width (depth) of the concentrated load, and C the length of the concentrated load.

When the beam is subjected to a set of equal and opposite transverse forces, there is a tendency to failure caused by stratification of the material. If this failure is restricted, then a shear stress τ is generated, defined as

$$\tau = \frac{QA_r}{I\sum\delta_i} \tag{4}$$

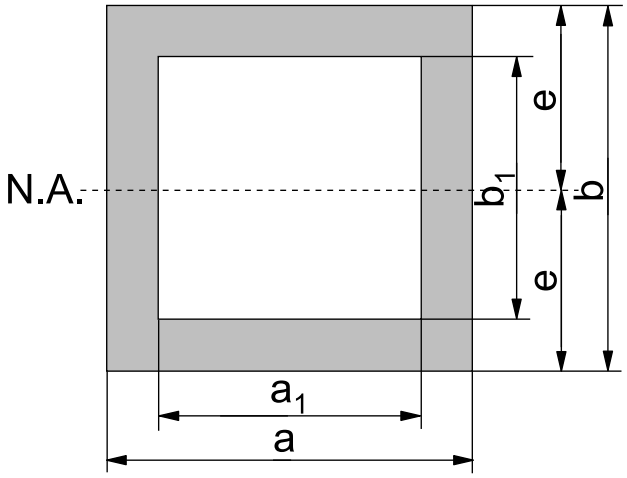

FIGURE 3. Cross section of the beam (view from waterside to landside).

with I the moment of inertia, Q the shear force, A_r the area of the cross section, and $\sum$ the summation. To calculate these parameters, it is necessary to analyze the cross section of the beam, which is a rectangular tube, as shown in Figure 3. Assuming that the beam is symmetric about the neutral axis passing through its centroid, we can calculate the relevant geometric parameters as

$$\begin{cases} A_r = ab - a_1b_1 \\ I = \dfrac{ab^3 - a_1b_1^3}{12} \\ Z = \dfrac{ab^3 - a_1b_1^3}{6b} \\ e = \dfrac{b}{2} \\ i = \sqrt{\dfrac{ab^3 - a_1b_1^3}{12(ab - a_1b_1)}} \end{cases} \tag{5}$$

where a and b are the length and width of the cross section, respectively; a_1 and b_1 are the internal length and width of

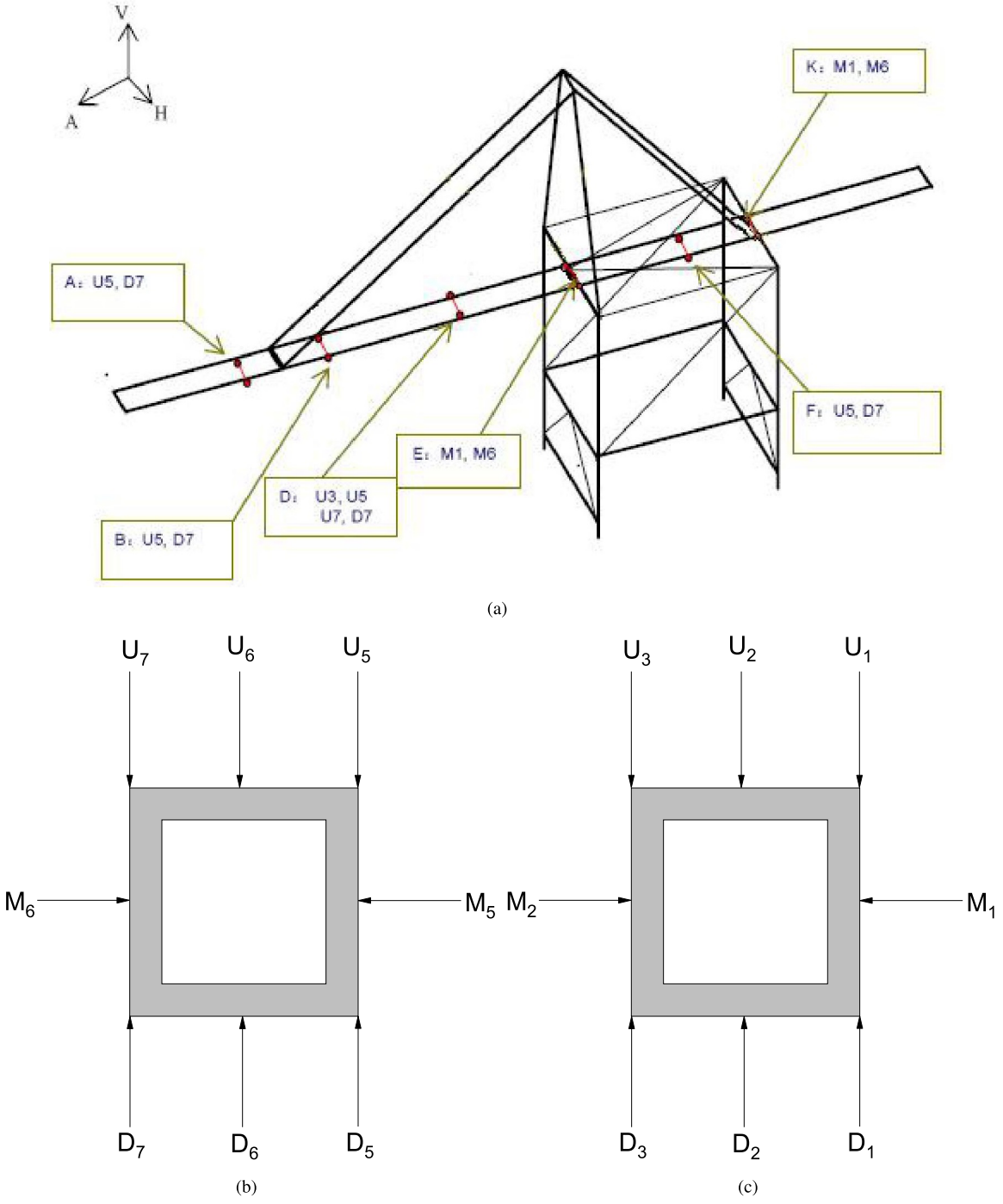

FIGURE 4. Positions of the measuring points Cross sections of left beam and right beam (view from waterside to landside).

the cross section, respectively; e is the extreme point; and i is the radius of gyration [15].

By calculating σ, we find that the maximum σ must appear at points C, D, E, F, or K (as shown in Figure 2). The sensors will be placed at these positions. Theoretically, the diagonal link connects with the beam at point C. However, in practice, the diagonal link connects with the beam at points A and B by lugs, so the sensors are set at the points A and B instead of point C.

All of the measurement points are shown in Figure 4. To reduce the number of sensors to 14, U_1, U_3, U_5, and U_7 (see Figure 4) are considered to have the same mechanical properties. Similarly, D_1, D_3, D_5, and D_7 are considered as the same. The same applies to M_1 and M_5, and M_2 and M_6. Therefore U_5 and D_7 are chosen as measurement points at A, B, D, and F; and M_1 and M_6 are chosen as measurement points at E and K. In addition, U_3 and U_7 are measured at point D to improve the measurement accuracy. These points

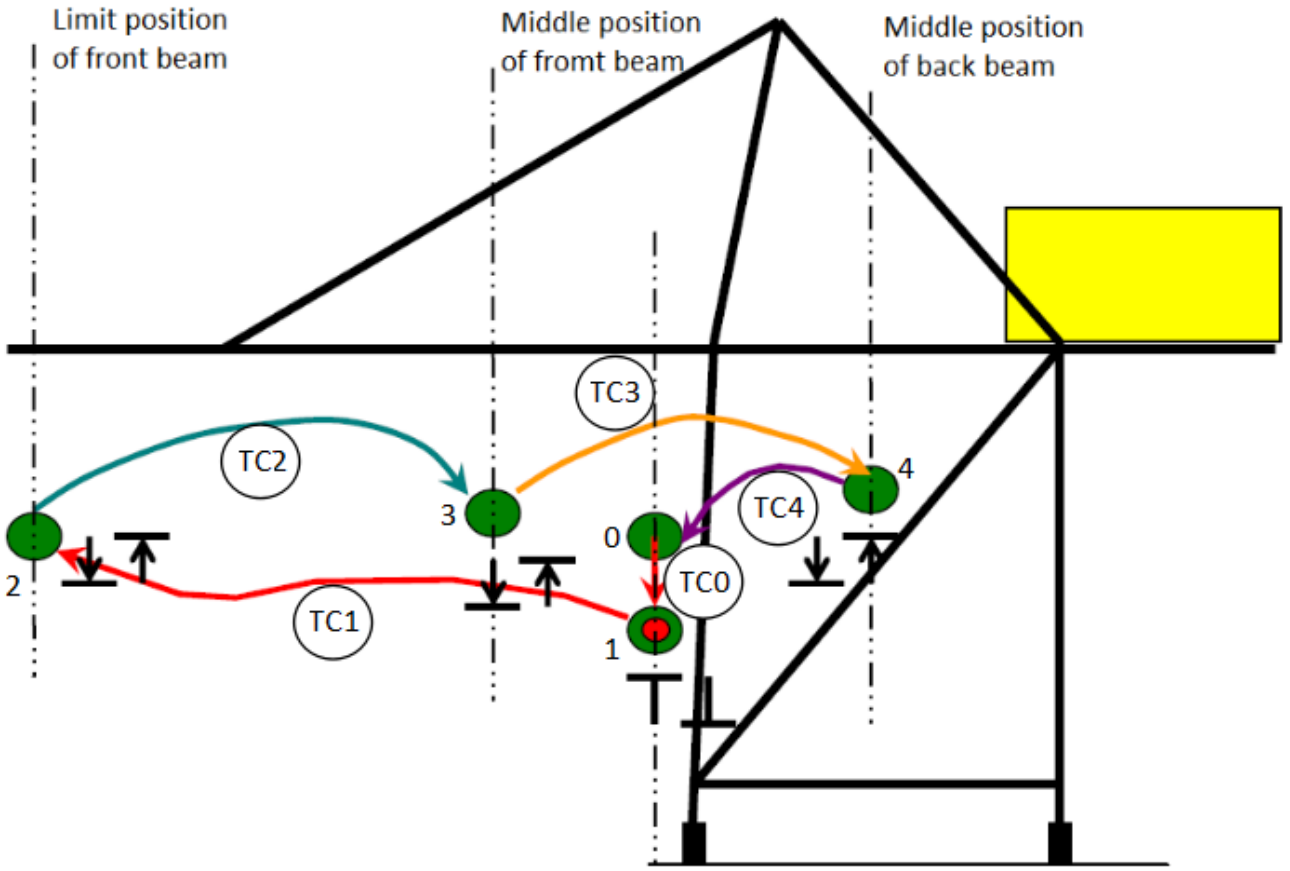

FIGURE 5. Schematic view of the positions with different loading and conditions.

have been labeled AU5, AD7, BU5, BD7, DU5, DU7, DD7, DU3, EM1, EM6, FU5, FD7, KM1, and KM6.

C. LOADING AND CONDITION

Main structure testing with dynamic load stress is based on a static stress test. With static stress tests, including quantitative distributions and static load waveforms [16], we can analyze the features of large static stress points in both amplitude and frequency domains, and then check the strength of the structure with a dynamic load.

The positions with different loading and conditions are shown in Figure 5. The test load is 25 tons (nominal load of 28 tons). The wind scale was 3 and the environmental temperature was 25°C. We have conducted a total of 10 cyclic experiments from testing condition 0 to testing condition 4, and calculated the average cycle time, which was 200 s.

The on-site test conditions (TC - Testing Condition) are:

1) TC0 (from position 0 to position 1): In this zero state condition, the test load is located in the hopper, and the grab bucket rests on the test load. The rope is loosened until there is no force between the trolley and the grab bucket.
2) TC1 (from position 1 to position 2): Firstly, the trolley runs at full speed to the limit position of the front beam and the grab bucket begins to free fall. Then, the control wire rope makes the bucket stop for 10 seconds, after which the bucket grabs the test load, and it begins to rise at full speed. Finally, the control wire rope makes the grab bucket stop.
3) TC2 (from position 2 to position 3): Firstly, the trolley runs to the middle position of the front beam and the grab bucket begins to free fall with the test load. Then, the control wire rope makes the bucket stop for 10 seconds, after which it begins to rise at full speed. Finally, the control wire rope makes the grab bucket stop.
4) TC3 (from position 3 to position 4): Firstly, the trolley runs to the position of the back beam and the grab bucket begins free fall with the test load. Then, the control wire rope makes the bucket stop for 10 seconds, after which it begins to rise at full speed. Finally, the control wire rope makes the grab bucket stop.
5) TC4 (from position 4 to position 0): The trolley runs back to the zero position of the beam. The grab bucket lays down the test load. The system goes back to zero and checks the zero drift of the test system.

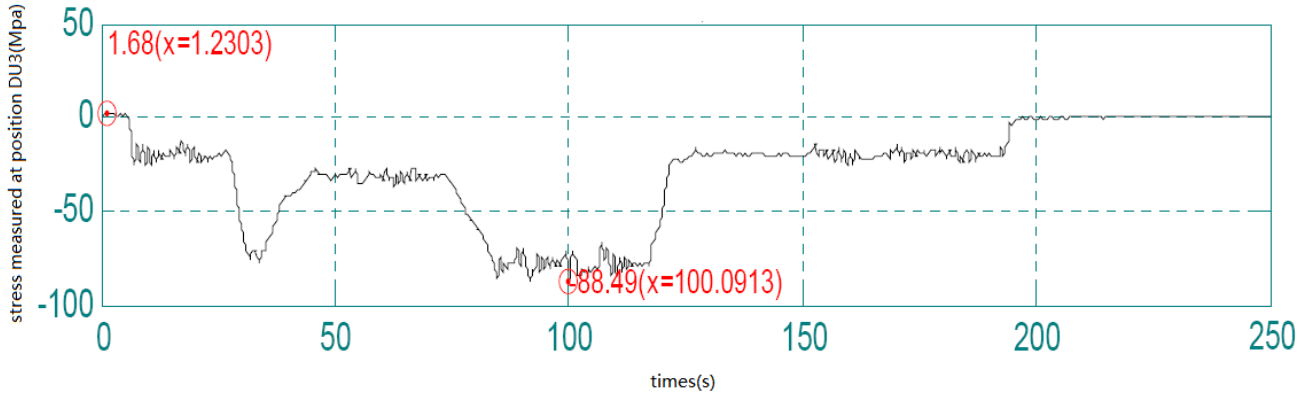

(a)

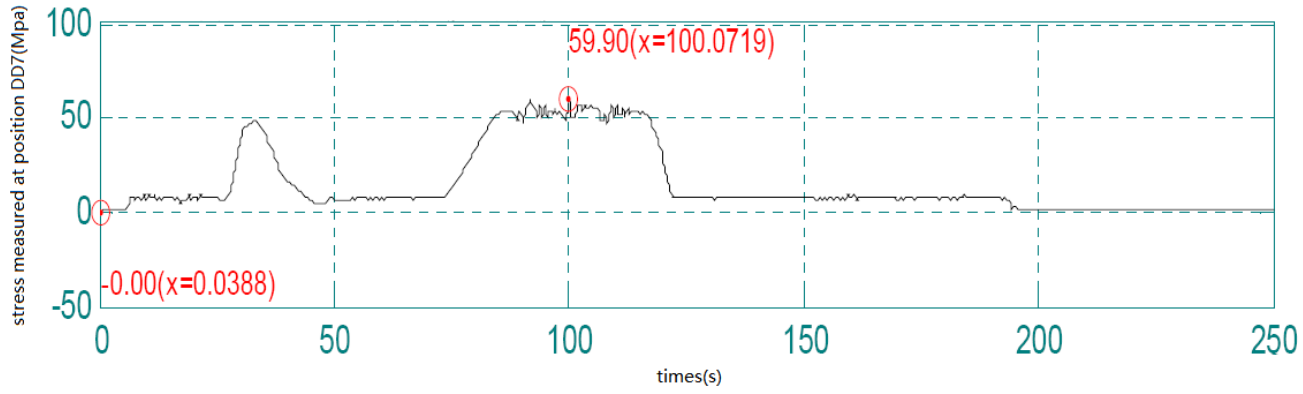

(b)

FIGURE 6. Time-domain curves of stress in maximum stress points.

III. RESULTS AND ANALYSIS

A. DATA COLLECTION

As described previously, data are collected from 14 sensitive points at varying positions along the beam and around the beam cross-section.

B. KALMAN FILTERING

The sampling rate of the signal voltages is 2500Hz. However, the field environment is complex, causing noise that interferes with the signal. To improve the efficiency of data analysis, it is necessary to process the data with a Kalman filter. The general linear discrete system can be expressed as

$$\begin{cases} X(k) = A(k)X(k-1) + B(k)U(k) + w(k) \\ Z(k) = H(k)X(k) + v(k) \end{cases} \tag{6}$$

where $X(k)$ is the n-dimensional state vector; $U(k)$ is the system control vector; $w(k)$ is the n-dimensional system noise vector; $A(k)$ is the state transition matrix from $k-1$ to k; $B(k)$ is the excitation transfer matrix from $k-1$ to k; $Z(k)$ is the m-dimensional observation vector; $H(k)$ is the output transfer matrix for time k; and $v(k)$ is the m-dimensional observation noise vector [17]. The Kalman filter is applied to data prediction, which requires the use of predictive derivation equations as follows:

$$\begin{cases} X(k|k-1) = A(k)X(k-1|k-1) + B(k)U(k) \\ P(k|k-1) = A(k)P(k-1|k-1)A(k)^T + Q(k) \\ X(k|k) = X(k|k-1) + K_g(k)(Z(k) - H(k)X(k|k-1)) \\ K_g(k) = P(k|k-1)H(k)^T(H(k)P(k|k-1)H(k)^T + R(k))^{-1} \\ P(k|k) = (I - K_g(k)H(k))P(k|k-1) \end{cases} \tag{7}$$

where $X(k|k-1)$ is the result of the prediction using the previous state of the system; $X(k-1|k-1)$ is the optimal result of the previous state of the system; $P(k|k-1)$ is the corresponding covariance of $X(k|k-1)$; $P(k-1|k-1)$ is the corresponding covariance of $X(k-1|k-1)$; A^T is the transpose of matrix A; $Q(k)$ is the covariance matrix of $w(k)$; $K_g(k)$ is the Kalman gain at time k; $R(k)$ is the covariance matrix of $v(k)$; and I is the unit matrix [18]. In this system, $x(k)$ represents the system status at time k, and $Z(k)$ represents the pressure measurement at time k, so $n = m = 1$, and the excitation transfer matrix $B(k)$ is a zero matrix. We have used Gaussian white noise as our model to better simulate the unknown real noise, which is often caused by a combination of many different sources of noise. If we increase the system noise, the Kalman gain will also increase, making the initial value more reliable; if we

increase the measured noise, the Kalman gain will decrease, making the theoretical value more reliable.

The data processed by Kalman filtering are shown in Figure 6. The horizontal axis is time in seconds, and the vertical axis is stress measured at positions DU3 and DD7 after filtering. We also label the maximum and minimum values after filtering.

C. CALCULATE THE MEASURED POINT STRESS

From the filtered signal, we can obtain the maximum value of stress at each stress measurement point and analyze the corresponding test condition. The calculation results for each measurement point are given in Table 1.

TABLE 1. Structural dynamic load strength (MPa).

Point	Max(MPa)	Time(s)	Min(MPa)	Time(s)
AU5	0	0	-40.09	159
AD7	17.34	41	0	0
BU5	0	0	-40.38	78
BD7	17.16	39	0	0
DU5	0.05	3	-82.60	84
DU7	0.55	2	-82.75	100
DD7	59.90	100	0	0
DU3	1.68	1	-88.49	100
EM1	8.39	91	-0.51	1
EM6	6.10	100	0	0
FU5	36.68	137	-4.40	35
FD7	0.01	4	-19.87	62
KM1	0	0	-4.63	62
KM6	2.67	159	-3.27	62

The results show that the maximum compressive stress occurs in condition TC2 (when the trolley runs to the middle position of the front beam), at DU3. The corresponding value is:

$$\sigma_{max}^{(DU3)} = -88.49 \quad (MPa)$$

The maximum tensile stress occurs also in condition TC2, at DD7. The corresponding value is:

$$\sigma_{max}^{(DD7)} = 59.90 \quad (MPa)$$

The STS crane beam is made of steel Q345 (Chinese criterion, similar to S355 in the European criterion, with the same dynamic safety factor), so the allowable stress is given by [15]:

$$[\sigma] = \sigma_y/n = 345/1.5 = 230 \quad (MPa)$$

where σ_y is the yield limit and n is the safety factor for the load. All of the measurement points with dynamic load stress should satisfy the strength requirements:

$$|\sigma|_{max} < [\sigma]$$

In field strength testing, the maximum tensile stress occurs at DD7, with a value of 59.90 MPa; the maximum dynamic load stress occurs at DU3 with a −88.49 MPa. These values meet the strength requirements.

IV. CONCLUSION

This paper introduces a systematic approach to analyzing the strength of the main structural component in an STS crane under dynamic load. Firstly, we have established a testing system for the main structural component in STS cranes, including signal sensing, conditioning, acquisition, and analysis. Secondly, we have identified the dangerous positions at which maximum stress may occur and arranged sensors in these positions. Thirdly, we have designed the on-site test conditions, and acquired signals and processed them with Kalman filter. Finally, we have calculated the stresses of the test positions under various test conditions.

However, there are some limitations of our method. Due to safety concerns, we have not conducted field tests under strong wind conditions. When strong winds occur, the structural connections of the crane (such as the connection between the legs and the main beam and the connection between the legs and the lower cross beam) can produce large eddy currents. Large negative pressures will be generated in this zone, creating a strong turbulent flow zone between the two main beams and producing a negative wind pressure.

REFERENCES

[1] N. Zrnić, D. Oguamanam, and S. Bošnjak, "Dynamics and modelling of mega quayside container cranes," *FME Trans.*, vol. 34, no. 4, pp. 193–198, 2006.

[2] Ü. N. Zrni and K. Hoffmann, "Development of design of ship-to-shore container cranes: 1959-2004," in *Proc. Int. Symp. Hist. Mach. Mech.*, 2004, pp. 229–242.

[3] H. H. Richardson, "Static dynamic load, stress, deflection cycles spur-gear system," M.S. thesis, Dept. Mech. Eng., Massachusetts Inst. Technol., Cambridge, MA, USA, 1958.

[4] N. Jones, "Plastic failure of ductile beams loaded dynamically," *J. Eng. Ind.*, vol. 98, no. 1, pp. 131–136, Feb. 1976.

[5] J. A. Laman, J. S. Pechar, and T. E. Boothby, "Dynamic load allowance for through-truss bridges," *J. Bridge Eng.*, vol. 4, no. 4, pp. 231–241, Nov. 1999.

[6] P. S. Shenoy and A. Fatemi, "Dynamic analysis of loads and stresses in connecting rods," *Proc. Inst. Mech. Eng., C, J. Mech. Eng. Sci.*, vol. 220, no. 5, pp. 615–624, May 2006.

[7] E. S. Hwang and A. S. Nowak, "Simulation of dynamic load for bridges," *J. Structural Eng.*, vol. 117, no. 5, pp. 1413–1434, May 1991.

[8] V. A. Kopnov, "Fatigue life prediction of the metalwork of a travelling gantry crane," *Eng. Failure Anal.*, vol. 6, no. 3, pp. 131–141, Jun. 1999.

[9] G. Hearn and R. B. Testa, "Modal analysis for damage detection in structures," *J. Structural Eng.*, vol. 117, no. 10, pp. 3042–3063, Oct. 1991.

[10] Q. Tran, J. Huh, V. Nguyen, C. Kang, J.-H. Ahn, and I.-J. Park, "Sensitivity analysis for ship-to-shore container crane design," *Appl. Sci.*, vol. 8, no. 9, p. 1667, Sep. 2018.

[11] Q. Tran, J. Huh, V. Nguyen, A. Haldar, C. Kang, and K. M. Hwang, "Comparative study of nonlinear static and time-history analyses of typical korean STS container cranes," *Adv. Civil Eng.*, vol. 2018, Aug. 2018, Art. no. 2176894.

[12] W. Johnson and S. L. Rice, "Impact strength of materials," *J. Appl. Mech.*, vol. 41, no. 2, p. 331, Arnold, 1972.

[13] M. F. Spotts, T. E. Shoup, and L. E. Hornberger, *Design of Machine Elements*, 8th ed. Upper Saddle River, NJ, USA: Prentice-Hall, 1978.

[14] S. W. Lee, J. J. Shim, D. S. Han, G. J. Han, and K. S. Lee, "An experimental analysis of the effect of wind load on the stability of a container crane," *J. Mech. Sci. Technol.*, vol. 21, no. 3, pp. 448–454, Mar. 2007.

[15] F. B. Seely, "Advanced mechanics of materials," *Phys. Today*, vol. 7, no. 4, pp. 26–27, 1954.

[16] G. Tang, X. Hu, W. Wang, T. H. Tang, C. Claramunt, and C. W. Chen, "Structural strength analysis of ship-to-shore crane," *Appl. Mech. Mater.*, vol. 858, pp. 34–37, Nov. 2017.
[17] Z. Wang, *Optimazation State Estimation System Identification*. Xian, China: Northwestern Polytechnical Univ. Press, 2004.
[18] M. S. Bartlett, "An introduction to stochastic processes, with special reference to methods and applications," *Technometrics*, vol. 65, no. 260, pp. 690–692, Aug. 1978.

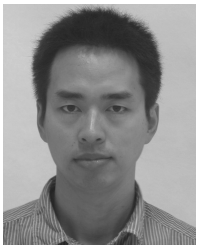

GANG TANG received the master's degree in mechanical engineering from the Harbin Institute of Technology, in 2007 and the Ph.D. degree in mechanical engineering from Shanghai Jiao Tong University, in 2011. He joined the Faculty at Shanghai Maritime University, where he is currently an Associate Professor with the Department of Mechanical Engineering. He has been in charge of more than ten Programs and participated in more than 15 Programs. He has published 36 papers and holds nine patents awarded. His research interest includes structural health monitoring.

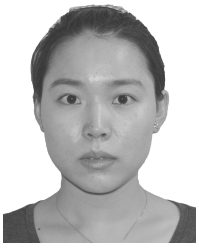

CHEN SHI is currently the graduate student with Shanghai Maritime University and pursuing the graduate degree in data science with Polytech Nantes, Nantes, France. She has a first-author conference Publication university. She has filed three invention patents and one international patent. She is currently working on the application of intelligent algorithms to cranes.

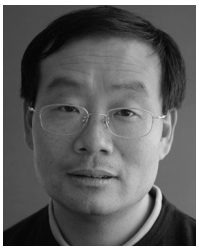

YIDE WANG received the B.S. degree in electrical engineering from the Beijing University of Post and Telecommunication, Beijing, China, in 1984, and the M.S. and Ph.D. degrees in signal processing and telecommunications from the University of Rennes, France, in 1986 and 1989, respectively. From 2008 to 2011, he was the Director of the Regional Doctorate School of Information Science, Electronic Engineering and Mathematics. He is currently a full-time Professor with Polytech Nantes (Ecole Polytechnique de l'université de Nantes). He is also the Director of research with Polytech Nantes. He is also in charge of the collaborations between Polytech Nantes and Chinese universities. He has authored or co-authored seven chapters in four scientific books, 50 journal papers, more than 100 national or international conferences. He has also coordinated or managed 15 National or European collaborative research programs. His research interests include array signal processing, spectral analysis, and mobile wireless communication systems.

XIONG HU received the bachelor's and Ph.D. degrees from Shanghai Jiao Tong University. He was a Visiting Professor of the Queensland University of Technology, Australia. He serves as the Executive Director of the Shanghai Mechanical Engineering Society, the Chairmen of the Committee of Equipment Condition Monitoring, Assessment and Strategic Decision of the Shanghai Mechanical Engineering Society, the Deputy Director of Branch of Health Condition Monitoring of Shanghai Equipment Management Association, and so on. He is currently a Professor and a Ph.D. Supervisor of Shanghai Maritime University (SMU), the Dean of Logistics Engineering College, SMU, and the Dean of the Sino-Dutch Mechatronics Engineering College, SMU. He was responsible for or participated in almost 100 research projects which were sponsored by National Funding Programs, government and both here and abroad enterprises, such as NNSF, 863 program, Dubai Aluminium Company Ltd., Port of Damman, Port of Shanghai, Shanghai Bao Steel Company, ZPMC, and BV. His current research interests include research and teaching works are included in (health) condition monitoring, (remote) control, (condition) assessment, and (maintenance) management of large equipment and its structure, and intelligent processing and prediction of health condition data and signals of machines. In recent years, his major research works are emphasized on the technique development and its application of health condition management, fault diagnosis, safety assessment, and integrated online system of the large hoisting appliances, such as cranes and logistics equipments.